A LINEAR INVERSION MODEL

FOR A DIRECTIONAL BOREHOLE RADAR

Koen W.A. van Dongen[(1)], **Peter M. van den Berg**[(2)], **Jacob T. Fokkema**[(3)]

[(1)] *Laboratory of Electromagnetic Research, Delft University of Technology,*
Mekelweg 4, 2628 CD Delft, The Netherlands,
E-mail: K.W.A.vanDongen@its.tudelft.nl

[(3)] *as* (1) *above, but E-mail: P.M.vandenBerg@its.tudelft.nl*

[(3)] *Section of Applied Geophysics, Delft University of Technology,*
Mijnbouwstraat 120, 2628 RX Delft, The Netherlands,
E-mail: J.T.Fokkema@citg.tudelft.nl

ABSTRACT

We discuss the imaging properties of a new directional borehole radar system. Directionality is obtained by shielding an electric dipole in one direction with a reflector. During the measurements the system rotates while it is pulled through a borehole. The changes in impedance as observed by the receiver, are formulated as a domain integral over the contrast times a sensitivity function. In order to obtain a 3D image of the subsurface, we linearize the integral equation and apply an inversion scheme in which we use the modelled radiation characteristics of the system.

INTRODUCTION

There is a great demand for methods to characterize the three dimensional (3D) subsurface. Therefore, various methods have been developed which probe the subsurface with seismic or electromagnetic waves from the surface. However, problems arise if the volume of interest is below an impenetrable layer or further away than the penetration depth. These problems are partly solved by measuring out of borehole near the region of interest. Unfortunately, with those systems, directionality is an offset against penetration depth. Hence, it is still hard to obtain 3D images, especially when the system has no directional sensitivity properties. However, we succeeded in the design of an antenna system, which combines a directional radiation pattern with sensitive receiving properties, and which fits in a single borehole [1], enabling us to obtain 3D images of the subsurface.

THE ANTENNA SYSTEM

A point in a Cartesian reference frame is denoted by the vector $\boldsymbol{x} = x_i$ for $i = \{1, 2, 3\}$ and in a circular cylindrical coordinate system by the vector $\boldsymbol{v} = v_i = \{x_1, r, \phi\}$. The x_i-component of the total electric wavefield is denoted as $\hat{E}^{\rm tot}_{x_i}(\boldsymbol{x})$, and satisfies in presence of a reflector

$$\hat{E}^{\rm tot}_{x_i}(\boldsymbol{x}) = \hat{E}^{\rm inc}_{x_i}(\boldsymbol{x}) + \hat{E}^{\rm rfl}_{x_i}(\boldsymbol{x}) \ , \tag{1}$$

where $\hat{E}^{\rm inc}_{x_i}$ is the field from the dipole antenna and $\hat{E}^{\rm rfl}_{x_i}$ the wavefield reflected at the surface $\mathbb{S}$ of the reflector. Note we use the symbol '$\hat{\ }$', to denote that a parameter is in the temporal Laplace domain, frequency domain results are obtained by taking the limit $s \to -i\omega$. Applying the boundary conditions at the surface of the perfectly conducting reflector, restricts the tangential components of the wavefields, viz.

$$-\hat{E}^{\rm inc}_{v_\alpha}(\boldsymbol{v}) = \hat{E}^{\rm rfl}_{v_\alpha}(\boldsymbol{v}), \qquad \forall\ \boldsymbol{v} \in \mathbb{S} \ , \tag{2}$$

where Greek subscripts are used to denote the tangential character, hence $\{\alpha, \beta\} = \{1, 3\}$. Neglecting the influence of the reflector on the electric current density at the dipole, we obtain the following integral equation

$$-\hat{E}^{\rm inc}_{v_\alpha}(\boldsymbol{v}) = \frac{1}{s\hat{\varepsilon}}\left[-\hat{\gamma}^2 I_{\alpha,i} + \nabla_{v_\alpha}\nabla_{v_i}\right]T^{-1}_{i,j}\int_{\boldsymbol{v}'\in\mathbb{S}} \hat{G}(\boldsymbol{v}|\boldsymbol{v}')T_{j,\beta}(\boldsymbol{v}|\boldsymbol{v}')\hat{J}^{\rm rfl}_{v_\beta}(\boldsymbol{v}')\mathrm{dA}(\boldsymbol{v}') \ , \tag{3}$$

where $\hat{J}^{\rm rfl}_{v_\beta}$ is the electric surface current density at the reflector, $T_{j,i}$ are the matrices to transform a vector from

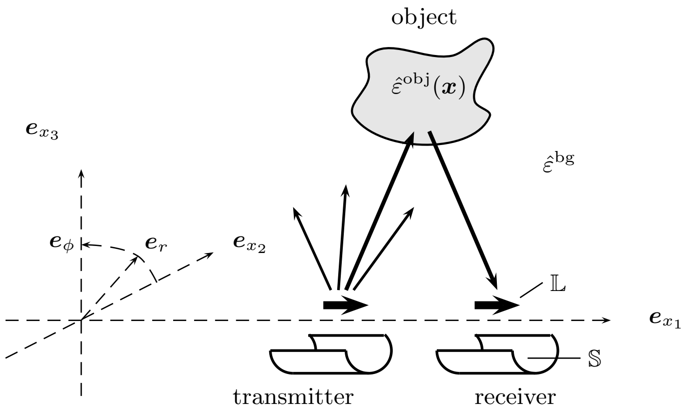

Fig. 1: The bistatic antenna setup positioned in both a Cartesian reference frame with unit vectors $\boldsymbol{e}_{x_i}$, and a circular cylindrical coordinate system with unit vectors $\boldsymbol{e}_{v_i}$. The object with complex medium parameter $\hat{\varepsilon}^{\mathrm{obj}}$is positioned in a homogenous medium described by $\hat{\varepsilon}^{\mathrm{bg}}$

the cartesian to a linear curved coordinate system and vice versa, $\hat{G}$ is Green's function, $\nabla_{v_\alpha}\nabla_{v_i}$ is the gradient-divergence operator, $I_{\alpha,i}$ is the identity operator, and where $\hat{\gamma}^2 = s^2\hat{\varepsilon}\mu_0$ with $\hat{\varepsilon}$ the complex permittivity and μ_0 the permeability of the medium. This integral equation is solved using a conjugate gradient method, [1] [3]. Using the solution in an integral representation over the reflector domain, enables us to compute the total electric wavefield. The results are used in an inversion process to obtain a 3D image of the subsurface, as described in the next section.

IMAGING

In order to obtain an image of the subsurface we formulate an integral equation. Solving this equation using standard and minimized back-propagation will result in an image of the subsurface.

Formulation of the Integral Equation

Reciprocity enables us to formulate an integral equation which connects the change of measured voltage at the receiver, $\delta\hat{V}^{\mathrm{rc}}$, with a contrast in the subsurface, $\delta\hat{\varepsilon} = \hat{\varepsilon}^{\mathrm{sct}} - \hat{\varepsilon}^{\mathrm{bg}}$, see [2], viz.

$$\delta\hat{V}^{\mathrm{rc}}(\boldsymbol{v}^{(k)}) = \hat{I}^{\mathrm{tm}} \int_{\boldsymbol{v}\in\mathbb{R}^3} \delta\hat{\varepsilon}(\boldsymbol{v})\hat{S}(\boldsymbol{v}|\boldsymbol{v}^{(k)})\,\mathrm{dV}(\boldsymbol{v}) \ , \tag{4}$$

where $\hat{I}^{\mathrm{tm}}$ is the transient electric current pulse at the transmitter, and where

$$\hat{S}(\boldsymbol{v}|\boldsymbol{v}^{(k)}) = -s\,\hat{e}^{\mathrm{tm}}_{v_k}(\boldsymbol{v}|\boldsymbol{v}^{(k);\mathrm{tm}})\,\hat{e}^{\mathrm{rc}}_{v_k}(\boldsymbol{v}|\boldsymbol{v}^{(k);\mathrm{rc}}) \ , \tag{5}$$

is the sensitivity function of the system, in which $\hat{e}^{\mathrm{tm}}_{v_k}$ and $\hat{e}^{\mathrm{rc}}_{v_k}$ are the wavefields caused by the transmitter and the receiver, positioned at $\boldsymbol{v}^{(k);\mathrm{tm}}$ and $\boldsymbol{v}^{(k);\mathrm{rc}}$ respectively. Computing the radiation patterns of one antenna at several radial distances and for several frequencies, we observe great similarities, see Fig. 2. Hence we approximate equation (5) by

$$\hat{S}(\boldsymbol{v}|\boldsymbol{v}^{(k)}) = -s\,\Gamma^2(\phi)\,\hat{e}^{\mathrm{dip}}_{v_k}(\boldsymbol{v}|\boldsymbol{v}^{(k);\mathrm{rc}})\,\hat{e}^{\mathrm{dip}}_{v_k}(\boldsymbol{v}|\boldsymbol{v}^{(k);\mathrm{rc}}) \ , \tag{6}$$

where Γ is the radiation pattern at a distance r_0 for the temporal frequency component f_0, and where $\hat{e}^{\mathrm{dip}}_{v_k}$ are the omnidirectional radiation patterns of a dipole. Since the system rotates around the x_1-axis, we introduce a discrete angular Fourier series with indices (n). Consequently, equation (6) reads in the angular Fourier domain

$$\delta\hat{V}^{\mathrm{rc;(n)}}(x_1,r) = \hat{I}^{\mathrm{tm}} \int_{x_1,r\in\mathbb{R}^3} \delta\hat{\varepsilon}^{(n)}(x_1,r)\,\hat{S}^{(n)}(x_1,r|x_1^{(k)},r^{(k)})\,\mathrm{d}x_1\,r\,\mathrm{d}r. \tag{7}$$

Solving the above equation for the unknown contrast $\delta\varepsilon^{(n)}$ in the angular Fourier domain and transforming the solution back to the spatial domain, results in an image of the subsurface.

Solution Method

An image is obtained by minimizing the error functional ERR for the unknown contrast $\delta\hat{\varepsilon}^{(n)}$, which satisfies

$$ERR^{(n)} = \sum_{x_1^{(k)}\in\mathbb{D}} \sum_{\omega_t\in\Omega} \left| \delta\hat{V}^{\mathrm{rc};(n)}(x_1^{(k)}) - \hat{I}^{\mathrm{tm}} \int_{x_1=-\infty}^{\infty} \int_{r=0}^{\infty} \delta\hat{\varepsilon}^{(n)}(x_1,r)\hat{S}^{(n)}(x_1,r|x_1^{(k)})\,\mathrm{d}x_1\,r\,\mathrm{d}r \right|^2 \Delta x_1 \Delta\omega \ , \quad (8)$$

Assuming $\delta\hat{\varepsilon}^{(n)}(x_1,r)$ to be frequency independent, we approximate the contrast by

$$\delta\hat{\varepsilon}^{(n)}(x_1,r) = \alpha^{(n)}\Delta\varepsilon^{(n)}(x_1,r) \ . \quad (9)$$

Hence we obtain $\Delta\varepsilon^{(n)}$ to be the update direction in the minimization procedure, viz.

$$\Delta\varepsilon^{(n)}(x_1,r) = \sum_{x_1^{(k)}\in\mathbb{D}} \sum_{\omega_t\in\Omega} \left(\hat{I}^{\mathrm{tm}}\hat{S}^{(n)}(x_1,r|x_1^{(k)})\right)^* \delta\hat{V}^{\mathrm{rc};(n)}(x_1^{(k)}) \ , \quad (10)$$

where the asterisk denotes that we take the complex conjugate. The update parameter $\alpha^{(n)}$ is given by

$$\alpha^{(n)} = \frac{\displaystyle\int_{x_1=-\infty}^{\infty}\int_{r=0}^{\infty} \left|\Delta\varepsilon^{(n)}(x_1,r)\right|^2 dx_1\,r\,dr}{\displaystyle\sum_{x_1^{(k)}\in\mathbb{D}} \sum_{\omega_t\in\Omega} \left| \hat{I}^{\mathrm{tm}} \int_{x_1=-\infty}^{\infty}\int_{r=0}^{\infty} \Delta\varepsilon^{(n)}(x_1,r)\,\hat{S}^{(n)}(x_1,r|x_1^{(k)})\,\mathrm{d}x_1\,r\,\mathrm{d}r \right|^2} \ . \quad (11)$$

Note that, taking $\alpha^{(n)} = 1$ a first image is obtained based on $\Delta\varepsilon^{(n)}$. We refer to this as standard back-propagation. In case we take $\alpha^{(n)}$ into account, we use the term minimized back-propagation.

Results

We tested two imaging procedures, standard and minimized back-propagation, on synthetic and measured data. Therefore we positioned two objects in a homogenous background medium, namely a deep water basin. Hence we use for the synthetic case and the sensitivity function, a non-conductive background medium with a relative permittivity similar to water, $\varepsilon_r = 80$. In addition, the transient generated wavefield has a center frequency of $f_0 = 100$ MHz. For this frequency Γ is computed at a radial distance of $r_0 = 0.3$ m. Finally, we only use the nine significant angular Fourier components around $n = 0$. The results are shown in Fig. 3.

CONCLUSION

Using reciprocity, a standard and minimized back-propagation method is derived, to image the subsurface using the voltage measured by the receiver. Both methods are tested, resulting in good images. The angular resolution increases if we use the minimized version. Since a limited number of angular Fourier components is used we save computational time and stabilize the process; however the angular resolution is limited.

ACKNOWLEDGEMENT

The authors wishes to thank R. van Waard and S. van der Baan from T&A Survey for their great support.

REFERENCES

[1] K.W.A. van Dongen, P.M. van den Berg, and J.T. Fokkema, "A Directional Borehole Radar: Numerical and Experimental Verification", *2001 IEEE AP-S International Symposium and USNC/URSI National Radio Science Meeting*, Boston, USA, July 8-13, 2001, Vol. II, ISBN 0 7803 7072 4, pp. 746-749.

[2] K.W.A. van Dongen, P.M. van den Berg, and J.T. Fokkema, "A three-dimensional imaging technique for a directional borehole radar", *SPIE's 46th Annual Meeting, Subsurface and Surface Sensing Technologies and Applications III*, July 30 - August 1, 2001, San Diego CA, USA, Vol. 4491, pp. 88-98.

[3] K.W.A. van Dongen, Ronald van Waard, Stefan van der Baan, P.M. van den Berg, and J.T. Fokkema, "A Directional Borehole Radar System", *Subsurface Sensing Technologies And Applications*, unpublished.

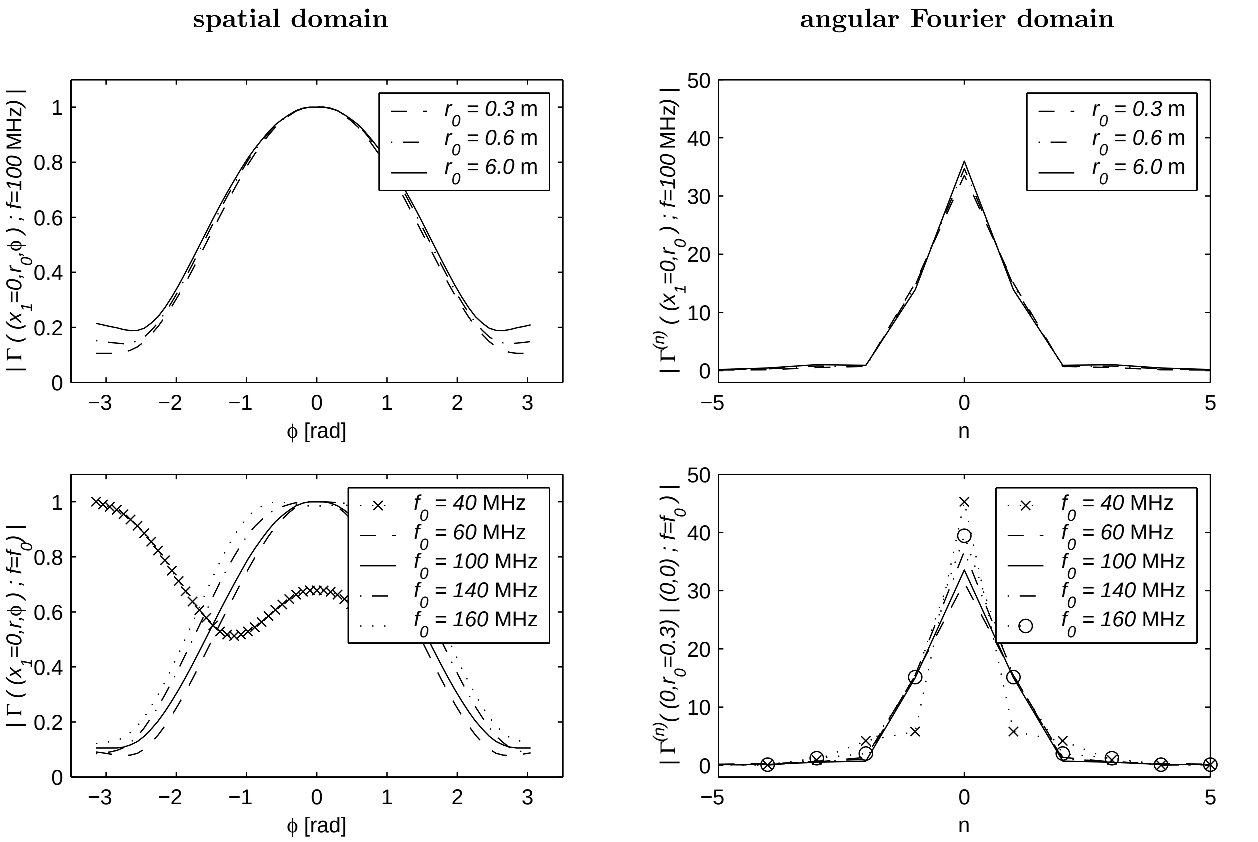

Fig. 2: The radiation pattern of the antenna system in the plane $x_1 = 0$ m, for various frequencies and at several radial distances.

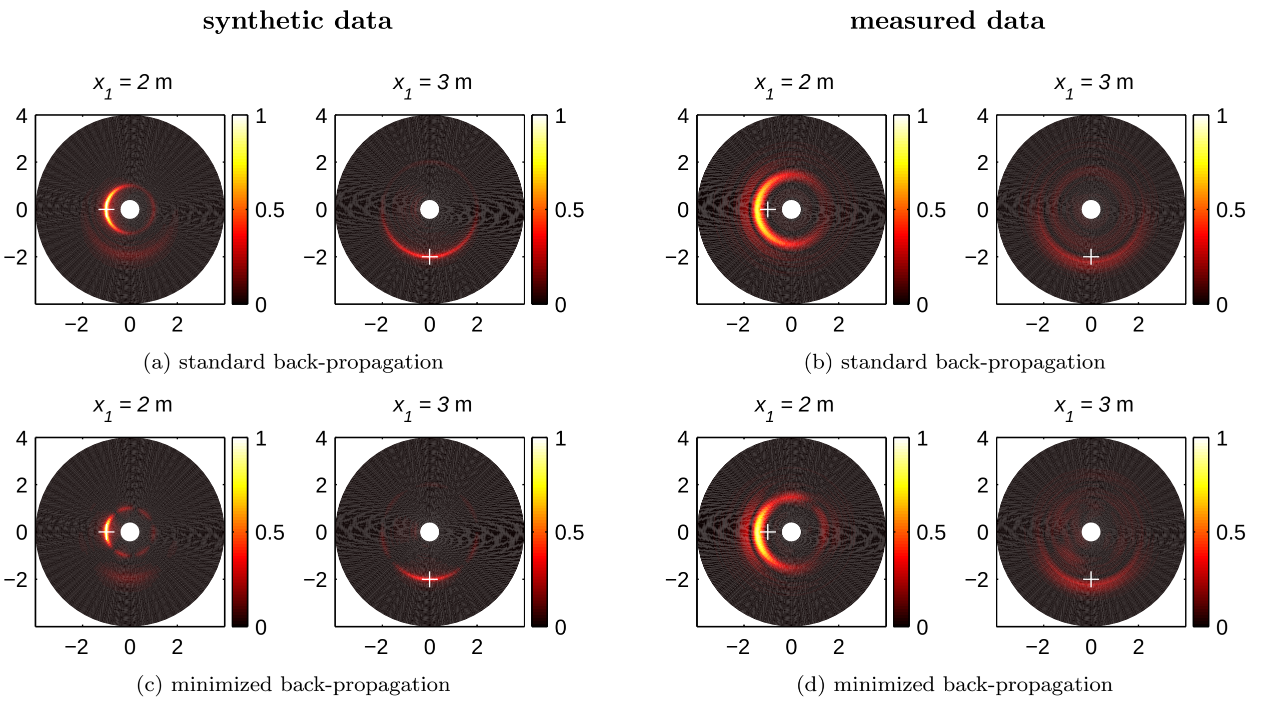

(a) standard back-propagation

(b) standard back-propagation

(c) minimized back-propagation

(d) minimized back-propagation

Fig. 3: Images of the subsurface in the planes $x_1 = 2.0$ m and $x_1 = 3.0$ m. The crosses indicate the object's positions